COBEM 2023 27TH INTERNATIONAL CONGRESS OF MECHANICAL ENGENEERING

ABCM Brazilian Society of Mechanical Sciences and Engineering
27th ABCM International Congress of Mechanical Engineering
December 04-08, 2023, Florianópolis-SC, Brazil

COB-2023-1486
Counterflow heat exchanger simulation with the Lattice-Boltzmann Method

Vinicius Akyo Matsuda
Ivan Talão Martins
Edilson Guimarães de Souza
Luben Cabezas Gómez
Heat Transfer Research Group, Department of Mechanical Engineering, São Carlos School of Enginnering, University of São Paulo, Trabalhador São-carlense Avenue, 400, 13566-970, São Carlos, SP, Brazil
viniciusmatsuda@usp.br
ivanmartins@usp.br
edilsongs@usp.br
lubencg@sc.usp.br

Abstract. *In this work the Lattice-Boltzmann Method (LBM) is used to simulate and study a simple counterflow heat exchanger. For this purpose, the D2Q9 dimensional LBM with single relaxation time, with the BGK (Bhatnagar-Gross-Krook) collision operator, was used. Two distribution functions were used, one for the Navier-Stokes equation, and the other for the energy conservation equation. An enthalpic based LBM was used to model the conjugate heat transfer between the fluids and the heat exchangers walls. Furthermore, the simulation results obtained with the LBM were compared against results derived from traditional simulation techniques. Performing this comparison, we expect to illustrate the capabilities of the LBM and demonstrate the impacts of the adopted hypotheses in common heat exchanger design simulation techniques. The results showed that inlet regions for both fluids exert a significant impact on the real effectiveness of the heat exchanger. Within these regions, the errors were the highest, showing the importance in simulating the non-developed thermal and flow regions. Although these higher errors mainly occurred in a small region of the heat exchanger, they were shown to build up to a few temperature degrees, indicating that they can impact on the correct design of the simulated devices.*

Keywords: *Lattice Boltzmann Method, Heat-Exchanger, Conjugate Heat Transfer, Dimensional LBM, Navier-Stokes.*

1. INTRODUCTION

In engineering fields, most problems related with heat transfer occur under conjugate heat-transfer conditions, such as in the case of this study about heat-exchangers. Thus, due to its application and importance, this problem is widely studied (Ma *et al.*, 2022; Aneesh *et al.*, 2016; Aakre *et al.*, 2023a). When using computational methods such as finite-difference, finite-volume, and finite element for conjugate heat-transfer (Roe *et al.*, 2008; Zhang *et al.*, 2012), a common approach is to apply iterative schemes on the interface, in which a Dirichlet condition is imposed for one side and a Neumann condition for the other. Then the heat transfer problem is separately solved for each side and the continuity at the interface is satisfied after a number of iterations, which can become difficult to satisfy for complicated interfaces.

On the other hand, the Lattice Boltzmann Method (LBM), which is a mesoscopic simulation technique that solves the Boltzmann equation on a discrete lattice (Succi, 2001), has some advantages when compared to traditional numerical methods. Some of these advantages are related to its ability to handle complex geometries, to simulate multiphase flows (Lee and Liu, 2010; Liang *et al.*, 2019) and conjugate heat-transfer (Korba *et al.*, 2020; Li *et al.*, 2014; Chen *et al.*, 2017), and for capturing non-equilibrium effects (Krüger *et al.*, 2017). Through the LBM, important performance parameters can be accurately predicted, such as heat transfer rates, pressure drop, temperature distributions, and overall efficiency of the device.

Heat exchangers, are fundamental devices in thermal engineering used to efficiently transfer heat from one fluid to another in the more simple case. They are essential components in various industries such as HVAC (heating, ventilation, and air conditioning), power generation, chemical processing, food production and processing, and others. Therefore, the optimization of such devices always has been an engineering necessity, being treated through the geometry and thermodynamic optimization. Recent works are dealing with the study of heat exchangers operating with super-critical fluids or liquid metals (Aakre *et al.*, 2023b; Lee *et al.*, 2017; Cong *et al.*, 2021). In such devices, the classical methods such as the effectiveness-NTU method, should be applied considering a discrete model due to the great variation of thermophysical properties with temperature. These models are complex and should include the simulation of heat transfer on the solid walls also. In these cases more exactly methods, such as convectional CFD or LBM could also be employed. However, as mentioned before, conjugate heat-transfer in conventional CFD often becomes difficult, necessitating iterative schemes,

but an LBM model can solve similar problem naturally.

In summary, this work seeks to perform a numerical analysis of a simple counter-flow heat-exchanger using the Lattice Boltzmann Method, and compare the given results with traditional simulation methods, such as the discrete effectiveness-NTU method. The chossen simulation configurations do not involve the simulation of super-critical fluids or liquid metals, but involve the simulation of low mass flow rates were the heat conduction in the solid wall is important, as well as, the variation of thermophysical properties with temperature. Although this work focus on a simple heat-exchanger configuration, which can in many cases, indeed be modeled through conventional means, we hope to show the capabilities of the LBM, in special for applications with lower mass flow rates and for microchannels.

The work is organized as follows: A brief mathematical description of the model adopted is given in Section 2. In Section 3. results regarding the simulation are shown and compared against a numerical solution with the effectiveness-NTU method. Finally, in Section 4. the main conclusion of this works are presented.

2. Numerical model

In this section the mathematical bases for performing the simulation are presented. The dimensional approach proposed by Martins *et al.* (2023) was used due to its facility to deal with more realistic scenarios, additionally, it removes the need to non-dimensionalize the macroscopic quantities into lattice units, thus removing a non trivial step from the problem solution.

2.1 Lattice Boltzmann method for fluid flow

For simulating the incompressible Navier-Stokes equation it was considered the traditional lattice Boltzmann equation (LBE) with the BGK (Bhatnagar *et al.*, 1954) collision operator. Giving a time and space discretization with the respective discrete intervals Δt and Δx, the LBE for the fluid flow is given by Eq. (1) (Krüger *et al.*, 2017), where f_i represents the density distribution function, f_i^{eq} is the equilibrium distribution function, τ stands for the relaxation time and $\mathbf{x}$ and t are the coordinate vector and time, respectively. The sub-index i represents each discrete velocity direction and $\mathbf{c_i}$ is the particle velocity vector in each direction.

$$f_i(\mathbf{x} + \mathbf{c_i}\Delta t, t + \Delta t) - f_i(\mathbf{x}, t) = -\frac{\Delta t}{\tau}\left[f_i(\mathbf{x}, t) - f_i^{eq}(\mathbf{x}, t)\right] \ . \tag{1}$$

Following Guo and Shu (2013), the equilibrium distribution functions for the fluid flow LBE are calculated by Eq. (2). In this equation $\mathbf{u}$ and ρ are the macroscopic velocity and density, respectively, c_s is the sound speed and w_i are the weights related with each velocity direction i. These last two variables depend on the velocity scheme considered.

$$f_i^{eq}(\mathbf{x}, t) = w_i \rho(\mathbf{x}, t)\left[1 + \frac{\mathbf{c}_i \cdot \mathbf{u}}{c_s^2} + \frac{(\mathbf{c}_i \cdot \mathbf{u})^2}{2c_s^4} - \frac{\mathbf{u} \cdot \mathbf{u}}{2c_s^2}\right]_{(\mathbf{x},t)} \ . \tag{2}$$

The $D2Q9$ velocity scheme was adopted in the simulations performed in this work. Thus, according to Qian *et al.* (1992) the velocity vectors and the associated weights are given by Eq. (3) and Eq. (4), respectively, considering $c = \Delta x/\Delta t$ and $c_s = c/\sqrt{3}$.

$$\mathbf{c_i} = c\begin{cases}(0,0), & i = 0,\\ (1,0),(0,1),(-1,0),(0,-1), & i = 1,...,4,\\ (1,1),(-1,1),(-1,-1),(1,-1), & i = 5,...,8.\end{cases} \tag{3}$$

$$w_i = \begin{cases}4/9, & i = 0,\\ 1/9, & i = 1,...,4,\\ 1/36 & i = 5,...,8.\end{cases} \tag{4}$$

Through the Chapman-Enskog analysis (Chapman and Cowling, 1952) the Navier-Stokes equations can be recovered from the LBE, and it can be shown that the LBE will correspond to the macroscopic Navier-Stokes equations if the relation between relaxation time, τ, and the kinematic viscosity, ν, is set as: $\nu = (\tau - 0.5\Delta t)c_s^2$.

The macroscopic quantities can be recovered from the distribution functions by its moments, being q the number of discrete velocity directions for the scheme chosen (for example, $q = 9$ for the $D2Q9$ scheme). These moments can be represented by the following expressions,

$$\rho(\mathbf{x},t) = \sum_{i=0}^{q-1} f_i(\mathbf{x},t), \tag{5}$$

$$\rho(\mathbf{x},t)\mathbf{u}(\mathbf{x},t) = \sum_{i=0}^{q-1} f_i(\mathbf{x},t)\mathbf{c_i}. \tag{6}$$

Regarding the boundary conditions (BC) it was implemented the bounce-back scheme for simulating the contact between the fluids and the tube walls, which correspond to the no-slip boundary condition. For the inlets a bounce-back scheme with the prescribed inlet velocity was used, while for the outlets with prescribed pressures, it was considered the anti-bounce-back scheme. For more details about the implementation of these conditions, see Krüger *et al.* (2017).

2.2 Lattice Boltzmann method for conjugate heat transfer

Accordingly to Korba *et al.* (2020), the two more accurate models to deal with the conjugate heat transfer with the LBM are the interface treatment model proposed by Li *et al.* (2014) and the enthalpy-based models (Rihab *et al.*, 2016; Chen *et al.*, 2017). In general, models that need a special interface treatment, have good precision, however, in the presence of boundaries with more complex geometries, or even in 3D configurations, their implementation can become difficult.

Otherwise, enthalpy-based models do not have to directly deal with the interfaces, as the heat transfer process trough the interface between the components occurs naturally, allowing their implementation for complicated geometries or even 3D configurations with easy. Furthermore, the accuracy of both methods in question are of second order when it is used the link-wise approach (see Krüger *et al.* (2017)) for the boundary nodes (Korba *et al.*, 2020). Thus, in this work, it will be used the enthalpy-based LBM proposed by Chen *et al.* (2017).

The energy conservation equation for a system composed by solid and an incompressible fluid without phase-change, and neglecting the viscous heat dissipation, heat generation and property variations with temperature, is given by Eq. (7) (Bird *et al.*, 2002).

$$\partial_t(\rho c_p T) + \nabla\cdot(\rho c_p T\mathbf{u}) = \nabla\left(k\nabla T\right) \tag{7}$$

Chen *et al.* (2017) defined a new variable $h_0 = (\rho c_p)_0 T$, being $(\rho c_p)_0$ a constant reference heat capacitance, which is defined as the average of the various heat capacitances of domain. Substituting $T = h_0/(\rho c_p)_0$ in Eq. (7) and defining $\sigma = \rho c_p/(\rho c_p)_0$, Eq. (8) can be obtained. For more details about the procedure, see Chen *et al.* (2017). As the original authors suggested in their paper, the therm $\partial_t\sigma$ is maintained in the equation and evaluated trough a simple forward Euler time discretization scheme.

$$\partial_t h_0 + \nabla\cdot(h_0\mathbf{u}) = \nabla\left(\frac{k}{\rho c_p}\nabla h_0\right) - \frac{k}{(\rho c_p)_0}\nabla h_0\nabla\left(\frac{1}{\sigma}\right) - \frac{h_0}{\sigma}\left[\partial_t\sigma + \mathbf{u}\cdot\nabla\sigma\right] \tag{8}$$

A distribution function g_i related to h_0 can be defined, resulting in the LBE with the dimensional approach (see Martins *et al.* (2023)) for the energy conservation is described by Eq. (9), and the equilibrium distribution function can be defined by Eq. (10). Note that, instead of the forcing scheme adopted by Chen *et al.* (2017), the proposed by Seta (2013) was used.

$$g_i(\mathbf{x}+\mathbf{c_i}\Delta t, t+\Delta t) - g_i(\mathbf{x},t) = -\frac{\Delta t}{\tau_T}\left[g_i(\mathbf{x},t) - g_i^{eq}(\mathbf{x},t)\right] + \left(1-\frac{\Delta t}{2\tau_T}\right)w_i\Delta t\left[S_g(\mathbf{x},t)\right] \tag{9}$$

$$g_i^{eq} = w_i h_0(\mathbf{x},t)\left[+\frac{\mathbf{c}_i\cdot\mathbf{u}}{c_s^2} + \frac{(\mathbf{c}_i\cdot\mathbf{u})^2}{2c_s^4} - \frac{\mathbf{u}\cdot\mathbf{u}}{2c_s^2}\right]_{(\mathbf{x},t)} \tag{10}$$

Performing the Chapman-Enskog analysis of Eq. (9) the relaxation time for the BGK collision operator, τ_T, is related with the thermal diffusivity $\alpha = k/(\rho c_p)$ such as $\alpha = (\tau_T - 0.5\Delta t)c_s^2$. Because the LBE without the source term recovers only the first term in the right hand side of Eq. (8), the other two ones must be included in the source term: $S_g = -\frac{k}{(\rho c_p)_0}\nabla h_0\nabla\left(\frac{1}{\sigma}\right) - \frac{h_0}{\sigma}\left[\partial_t\sigma + \mathbf{u}\cdot\nabla\sigma\right]$.

Following the definition of heat flux from Karani and Huber (2015), for the BGK collision operator we have:

$$-\frac{k}{(\rho c_p)_0}\nabla h_0 = -\sigma\frac{k}{\rho c_p}\nabla h_0 = \sigma\left(1-\frac{\Delta t}{2\tau_T}\right)\sum_i \left[g_i - g_i^{eq}\right]\mathbf{c_i}, \tag{11}$$

The spatial derivatives of σ and $1/\sigma$ can be evaluated by a isotropic scheme as $\nabla\chi(\mathbf{x},t) = (c_s^2\Delta t)^{-1}\sum_i w_i\chi(\mathbf{x}+\mathbf{c_i}\Delta t, t+\Delta t)\mathbf{c_i}$, see Succi (2001). For the time derivative, as suggested by Chen *et al.* (2017), it is possible to use the Euler's scheme $\partial_t(\mathbf{x},t) = [\sigma(\mathbf{x},t) - \sigma(\mathbf{x},t-\Delta t)]/\Delta t$. Thus, the source term can be reorganized as shown in Eq. (12).

$$\begin{aligned} S_g = {} & \frac{1}{c_s^2\Delta t}\sigma\left(1-\frac{\Delta t}{2\tau_T}\right)\left[\sum_i (g_i - g_i^{eq})\,\mathbf{c_i}\right]\cdot\left[\sum_i w_i\frac{1}{\sigma(\mathbf{x}+\mathbf{c_i}\Delta t, t+\Delta t)}\mathbf{c_i}\right] \\ & -\frac{h_0}{\sigma}\left[\frac{\sigma(\mathbf{x},t)-\sigma(\mathbf{x},t-\Delta t)}{\Delta t} + \frac{1}{c_s^2\Delta t}\mathbf{u}\cdot\sum_i w_i\sigma(\mathbf{x}+\mathbf{c_i}\boldsymbol{\Delta t}, \mathbf{t}+\boldsymbol{\Delta t})\mathbf{c_i}\right], \end{aligned} \tag{12}$$

Finally, the macroscopic temperature can be obtained by the zero order moment of the distribution function as follows,

$$T(\mathbf{x},t) = \frac{1}{(\rho c_p)_0}\left[\sum_{i=0}^{q-1} f_i(\mathbf{x},t) + \frac{\Delta t}{2}S_g(\mathbf{x},t)\right], \tag{13}$$

Regarding the boundary conditions it was implemented the bounce-back scheme for external heat-exchanger walls, which correspond and adiabatic boundary condition. For the inlets a anti-bounce-back scheme with the prescribed inlet temperatures was used, while for the outlets with prescribed pressures, it was considered the anti-bounce-back scheme. For more details about the implementation of these conditions, see Krüger *et al.* (2017).

3. Results

3.1 1D heat diffusion between two solids

First, as a benchmark problem, a one-dimensional conduction between two different solids is carried out. A square domain with side $L = 0.50\ m$ is considered, being the left half occupied by copper and the right, by silicon. Thus, the interface is located at $x_i = 0.25\ m$. The left wall is maintained at $T_{w_l} = 313.15\ K$ and the right wall is kept at a constant temperature of $T_{w_r} = 293.15\ K$.

The copper and silicon properties are assumed to be constants, measured at $293.15\ K$, being $k_{Cu} = 401.2\ Wm^{-1}K^{-1}$, $c_{p_{Cu}} = 384.5\ Jkg^{-1}K^{-1}$ and $\rho_{Cu} = 8934.0\ kgm^{-3}$ for copper and $k_{Si} = 149.6\ Wm^{-1}K^{-1}$, $c_{p_{Si}} = 709.1\ Jkg^{-1}K^{-1}$ and $\rho_{Si} = 2330.0\ kgm^{-3}$ for silicon. The simulation is performed using a two-dimensional velocity scheme, the $D2Q9$. Thus, the top and bottom walls are assumed insulated, to kept the results the same as the one-dimensional problem.

The analytical solution for the temperature profile at steady-state can be given by Eq. (14).

$$\begin{cases} T(x) = T_{w_l} + x\cdot\left[\frac{T_{w_r}-T_{w_l}}{x_i + \frac{k_{Cu}}{k_{Si}}\cdot(L-x_i)}\right], & \text{if } 0 < x \leq x_i; \\ T(x) = T_{w_r} - (L-x)\cdot\frac{k_{Cu}}{k_{Si}}\left[\frac{T_{w_r}-T_{w_l}}{x_i + \frac{k_{Cu}}{k_{Si}}\cdot(L-x_i)}\right], & \text{if } x_i \leq x < L; \end{cases} \tag{14}$$

The numerical simulation was performed considering $\Delta t = 2.5\cdot 10^{-3}\ [s]$ and $\Delta x = 2.5\cdot 10^{-3}\ [m]$. The simulated and analytically obtained results are shown in Fig. 1a). A simple qualitative analysis shows that the employed model can capture with very good accuracy the system steady-state behavior. In fact, the maximum relative error was equal to 0.0001%, as shown in Fig. 1b). These results indicate that the implemented method can be applied for simulating conjugate heat transfer problems with confidence.

3.2 Heat-Exchanger with a flat-thin interface

In this section a counter-flow heat-exchanger, with water at atmospheric pressures, P_{atm}, considered as the flowing fluid at both sides is simulated. A schematic of the simulated problem is shown in Fig. 2, where $H = 0.002m$, $L = 0.02m$, $T_{in_1} = 20°C$ and $T_{in_2} = 80°C$. For the solution of this problem, it was supposed a rectangular channel where the length in the third $\mathbf{k}$ direction is far greater than the channel height, eliminating the border effect in this direction and allowing a

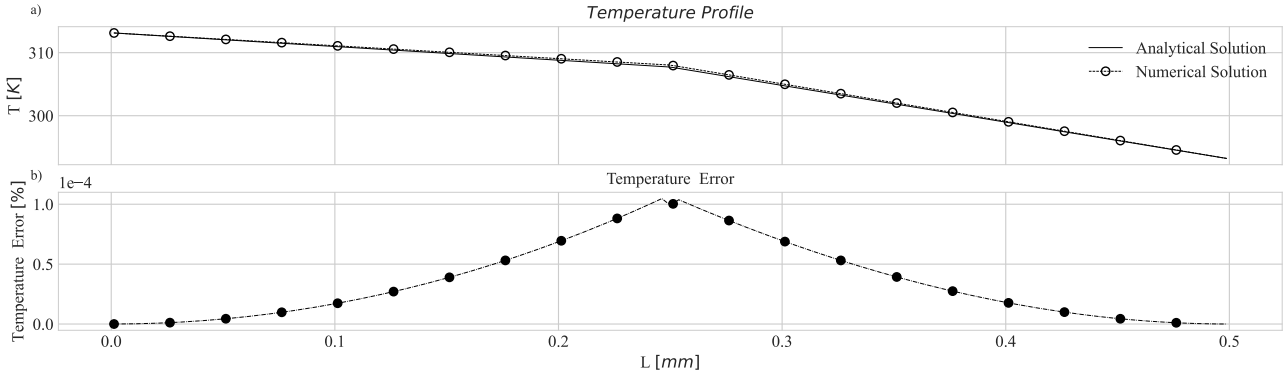

Figure 1. Comparison - LBM vs Analytical: a) Temperature profiles; b) Relative errors.

2D modeling of the problem. Besides that, the interface between the fluids are assumed to be thin, with high conductivity and negligible capacitance, excluding in this way the wall influence of the model. The simulations were performed for $\Delta t = 5.0 \cdot 10^{-6}\ [s]$ and $\Delta x = 4.0 \cdot 10^{-5}\ [m]$. Additionally, a solution for the temperature profiles, according to the Discretization into Sub-Heat Exchanger Method (DSHM) (Nellis and Klein, 2008), was obtained.

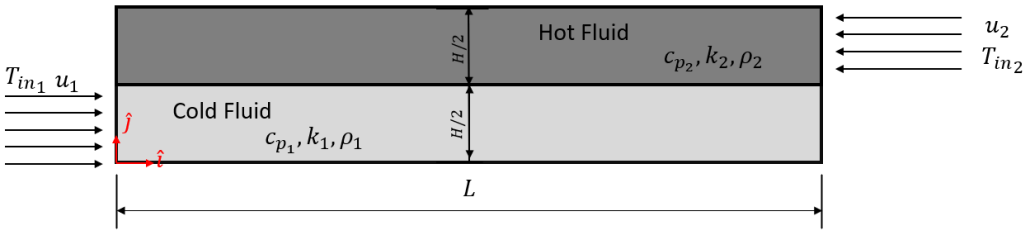

Figure 2. Heat-Exchanger Model.

In total, four different simulations were performed, and the results regarding the fluids temperature distribution and the total heat exchanged in the form of total mean relative errors, given by Eq. 15, between the LBM and the DSHM solutions, are shown in Tab. 1. The data presented, shows that the errors will tend to grow with mass flux in each channel. These results show the influence of the thermal entrance region in this heat exchanger configuration. This region is known to be proportional to the product of the Reynolds and Prandtl numbers (Lienhard and Lienhard, 2020), as shown in Eq. (16), and therefore, it is expect to grow with the mass flux.

$$Error = 100\% \left[\sqrt{\frac{\sum (T_{DSHM} - T_{LBM})^2}{\sum T_{LBM}^2}} \right] \tag{15}$$

$$\frac{x_{entry}}{D_h} = \alpha Re_{D_h} Pr \tag{16}$$

Rearranging Eq. (16), and estimating the percentage of the heat-exchanger length that the flow takes to be thermally fully developed, the coefficient of proportionality, α, as given in Lienhard and Lienhard (2020), is set to be 0.034 for a constant wall temperature and 0.043 for a constant wall heat flux, and so it can be assumed to be of the order of 10^{-2}. In this case, it will be used to give us an order of magnitude of the entrance region relative length. These results are shown in Table 2.

As it can be seen, as the inlet velocity of the heat-exchanger channels grows, the entrance region starts to take a non negligible portion of the total length, reaching about 10% of the total length, for $u_{in} = 0.02\ ms^{-}1$. In this condition the hypotheses of totally developed flow starts to lose its coherence, and therefore other design methods must used, such as the the LBM, to efficiently model the problem.

Figure 3 a), shows a graphical comparison between the temperature profiles obtained both with the LBM and DSHM for the Condition 4. It is noticeable that both methods present similar results, with the same overall behavior for the axial variation of temperatures. However due to the entrance effects of flow development, the higher errors are generated mostly on the entrance regions, where the flow is still developing, as shown in Fig. 3 b). As pointed out in Lienhard and Lienhard (2020), these regions present higher Nusselt number values, and therefore, will transfer more heat, increasing the temperature variations within these regions.

Table 1. Relative Errors LBM vs DSHM.

	Condition 1	**Condition 2**	**Condition 3**	**Condition 4**
$u_1\ [ms^-1]$	0.0025	0.005	0.01	0.02
$u_2\ [ms^-1]$	0.0025	0.005	0.01	0.02
$Error\ T_1\ [\%]$	0.28	0.49	0.73	0.96
$Error\ T_2\ [\%]$	0.24	0.41	0.60	0.79
$Error\ T_{1_{out}}$	0.44	0.80	1.21	1.57
$Error\ T_{2_{out}}$	0.45	0.78	1.12	1.41
$Error\ Q\ [\%]$	0.03	0.09	0.22	0.49

Table 2. Entrance Region relative length.

	Condition 1	**Condition 2**	**Condition 3**	**Condition 4**
$x_{in_{cold}}/L$	0.01	0.03	0.06	0.12
$x_{in_{hot}}/L$	0.01	0.03	0.06	0.11

3.3 Heat-Exchanger with a non-negligible interface

In addition, a second configuration for the counter-flow heat-exchanger is simulated. Differently from the previous model, the solid wall that separates the two fluid streams now has a finite thickness, $t = 0.0002m$. The simulated heat-exchanger is shown in Fig. 4, where $H = 0.001m$, $L = 0.01m$, $T_{in_1} = 20°C$ and $T_{in_2} = 80°C$. To test the influence of the wall in the models, are considered four different wall materials, see Tab. 3, and the inlet velocities are set as $u_1 = u_2 = 0.005\ ms^{-1}$, for mitigating the effects of the entrance regions. All wall properties are assumed to be constants and measured at $293.15\ K$. The other simplifying hypotheses and conditions are the same as for the previous tests. The simulations were performed for $\Delta t = 5.0 \cdot 10^{-6}\ [s]$ and $\Delta x = 2.0 \cdot 10^{-5}\ [m]$.

Table 3. Wall properties for different materials.

	Copper	**Aluminum**	**Silicon**	**Steel AISI 304**
$k_w\ [Wm^{-1}K^{-1}]$	401.2	237.0	149.6	13.8
$c_{p_w}\ [Jkg^{-1}K^{-1}]$	384.5	905.0	709.1	400.0
$\rho_w\ [kgm^{-3}]$	8934.0	2707.0	2330.0	8000.0

The results regarding the total mean relative errors, calculated by Eq. 15, between LBM and DSHM are shown in Tab. 4. In general, the results showed good agreement with the DSHM method, presenting overall low errors between the solutions, and correctly predicting the temperature profiles and the total heat-exchanged between the fluids. As the conductivity of the wall, k_w, increases a rise in the generated errors can be observed, and also a heat-exchanger effectiveness, ϵ, decrease is predicted by the LBM, as shown in Tab. 5. These errors will occur due to the presence of axial, i.e., longitudinal heat conduction in the solid wall, which can greatly impact the overall performance of these devices (Nellis and Klein, 2008).

This effect, can be quantified by a quantity called "Axial Conduction Parameter", denoted by λ, and given by Eq. (17), which relates the rate of heat transfer along the length of the heat-exchanger in the solid wall due to the axial conduction to the rate of heat transfer between the streams (Nellis and Klein, 2008). The effect of conduction in the longitudinal direction in the stream with respect to the rate of heat transfer by advection in the stream, is proportional to the inverse of Peclet number square, Pe, defined by Eq. (18) (Nellis and Klein, 2008).

$$\lambda = \frac{1}{R_{ac}(c_p\dot{m})|_{min}} = \frac{k_w(tH)}{L(c_p\dot{m})|_{min}} \tag{17}$$

$$Pe_{Dh} = Re_{Dh}P_r \tag{18}$$

Table 6 shows the Axial Conduction Parameter and the Peclet number for the different cases studied in this section. In general it is possible to see that in the given condition the Pe is sufficiently large and presents a small variation for the studied cases, so that the longitudinal condition in the stream is of little significance in relation to the advection. The errors obtained and shown in Tab. 4, are related to the results presented in Tab. 6, where it is shown that the copper wall

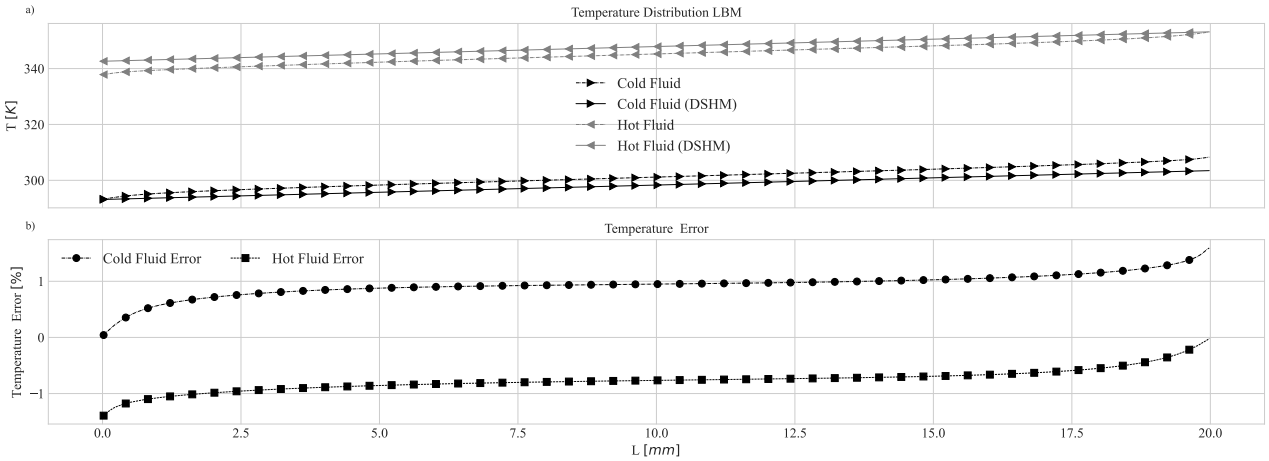

Figure 3. Condition 4 - LBM vs DSHM: a) Temperature profiles; b) Relative errors.

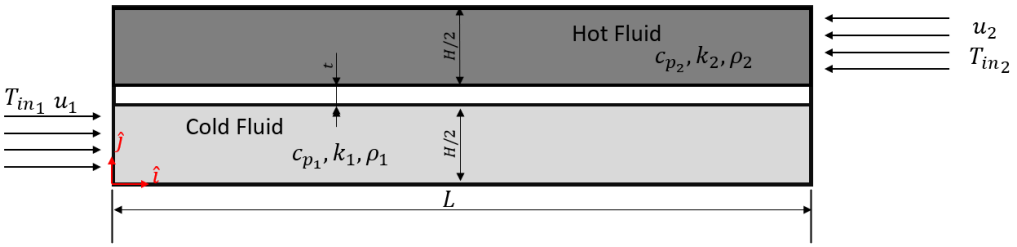

Figure 4. Heat-Exchanger Model.

will generate more errors, principally for the prediction of the outlet temperature, due to the obtained higher value for λ. In this case a more complex model is indeed required for the simulation of this small heat exchanger where the axial conduction takes a meaningful role in the process, largely impacting the behaviors and the performance of the device.

Figure 5 a), shows the mean temperature profiles for each region (Hot Fluid, Solid Wall and Cold Fluid), and the results obtained trough the heat-exchanger discretization method. Differently for what is observed in Fig. 3, a higher "temperature jump" starts to occur on both inlets, which is characteristic of significant but not dominant effects of axial conduction. Additionally the "ideal" model derived from traditional design methods, which does not take into account the wall thermal conductivity influence, starts to predict better performance, or in other words, a greater ΔT between inlets and outlets. These errors, shown both in Table 4 and Fig. 5 b) surpass the errors generated by the entrance region effects, and are expected to become even higher as the the mass flow diminishes.

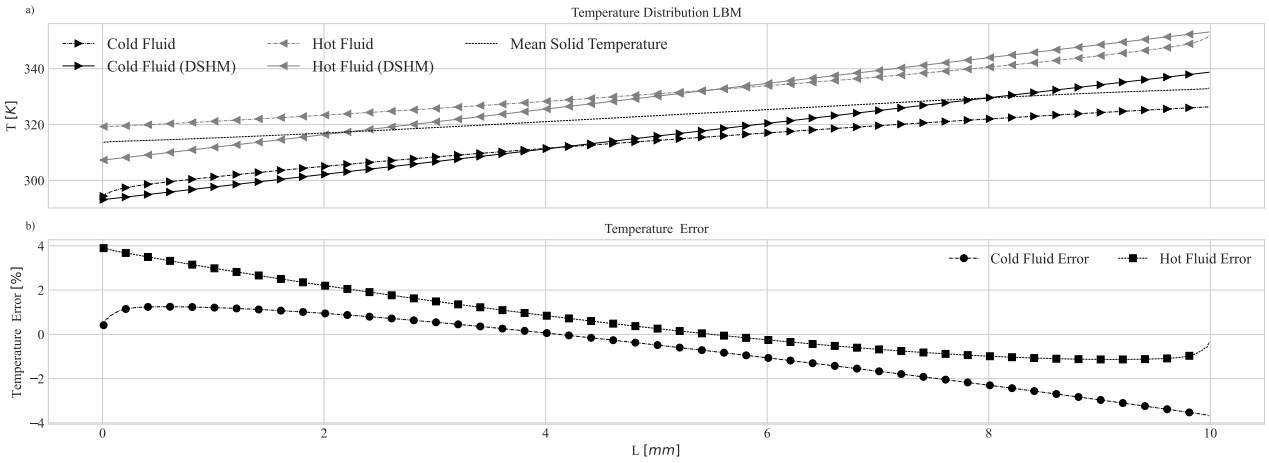

Figure 5. Copper Wall - LBM vs DSHM: a) Temperature profiles; b) Relative errors.

Finally, to illustrate this problem, a simulation with the same configuration and conditions, but setting $u_1 = u_2 =$

Table 4. Relative Errors between LBM and DSHM for a finite solid wall.

	Copper	**Aluminum**	**Silicon**	**Steel AISI 304**
$Error\ T_1\ [\%]$	1.7	1.7	1.8	1.5
$Error\ T_2\ [\%]$	1.6	1.4	1.3	1.2
$Error\ T_{1_{out}}$	3.8	3.6	3.6	2.4
$Error\ T_{2_{out}}$	3.8	3.4	3.1	2.2
$Error\ Q\ [\%]$	0.3	0.2	0.2	0.1

Table 5. Effectiveness: LBM vs DHSM.

	Copper	**Aluminum**	**Silicon**	**Steel AISI 304**
$\epsilon_{LBM}\ [\%]$	54.5	56.7	58.2	64.1
$\epsilon_{DSHM}\ [\%]$	76.5	76.5	76.5	76.1

Table 6. Axial Conduction Parameter.

	Copper	**Aluminum**	**Silicon**	**Steel AISI 304**
λ	0.38	0.23	0.14	0.01
Pe_{cold}	23.4	23.4	23.5	23.5
Pe_{hot}	22.1	22.1	22.1	22.0

$0.001\ ms^{-1}$, which results in $\lambda = 1.89$ was performed. The results are presented in Figs. 7 and 6. In this case the energy transferred through the longitudinal direction is an important contribution to the overall performance of the heat exchanger. Overall, a great reduction in the performance is seen, as expected for a case were the conduction in the longitudinal direction is relevant. Now the temperature difference between inlet and outlet simulated with the LBM is greatly reduced, when compared to the discrete model.

Additionally, Fig. 7 shows a temperature map for the heat-exchanger model. It is noticeable from it, that the temperature gradients will be more concentrated in the inlet regions (closer isothermal lines), showing the called "Temperature Jumps" in these regions, while for the rest of the heat-exchanger length it will tend to be more constant.

4. Conclusion

In the present work, the Lattice-Boltzmann Method was used to simulate and study a simple counter-flow heat-exchanger, considering the dimensional LBM with the BGK single relaxation time model. Two distribution function were used to correctly model the problem, one for modeling the incompressible Navier-Stokes equation for the fluid streams, and the other for modeling the energy conservation equation in the whole heat exchanger. This was accomplished by the use of enthalpic based LBM that allowed to model the conjugate heat transfer between the fluids and between the fluids and solid. A benchmark test with analytical solution was performed and the employed model was shown to be able to predict the resulting temperature profiles, validating both the model and its implementation.

In sequence, results regarding the simulation of a simple heat-exchanger model were presented. First, a heat-exchanger with rectangular channel with a flat-thin interface was studied. Although simple, these simulations allowed us to study the effect of the entrance region, both thermal and hydrodynamic, on the heat exchanger behavior. The LBM model was shown to be able to capture the thermal and hydrodynamic development regime of the flow within the development region. In this region were obtained the highest relative errors between the LBM and discrete methods, showing the importance of simulating the non-developed thermal and flow regions. Although these higher errors mainly occurred in a small region of the heat exchanger, they were shown to build up to a few temperature degrees, indicating that they can impact on the correct design of the simulated devices.

Additionally, a second heat-exchanger configuration with a finite solid wall was simulated to study the solid wall effects on the heat exchanger behavior. In total, four materials with highly different thermal conductivity were tested. The materials with lower conductivity lead to LBM simulation results similar to the ones obtained with the discretization method. This was an expected behavior, since for this condition the Axial Conduction Parameter were low, and therefore the energy transferred in the longitudinal direction trough the solid wall was negligible. As this parameter increased, this portion starts to be relevant and the employed discrete model loosed its accuracy and the LBM produced more coherent results. This indicates to the necessity of considering these effects for a correct project of the studied type of devices.

In conclusion, the modeling and simulation of heat-exchanger trough the LBM has been shown to posses good accuracy when compared to traditional methods, being applicable for a variety of cases. Furthermore, it was shown to be

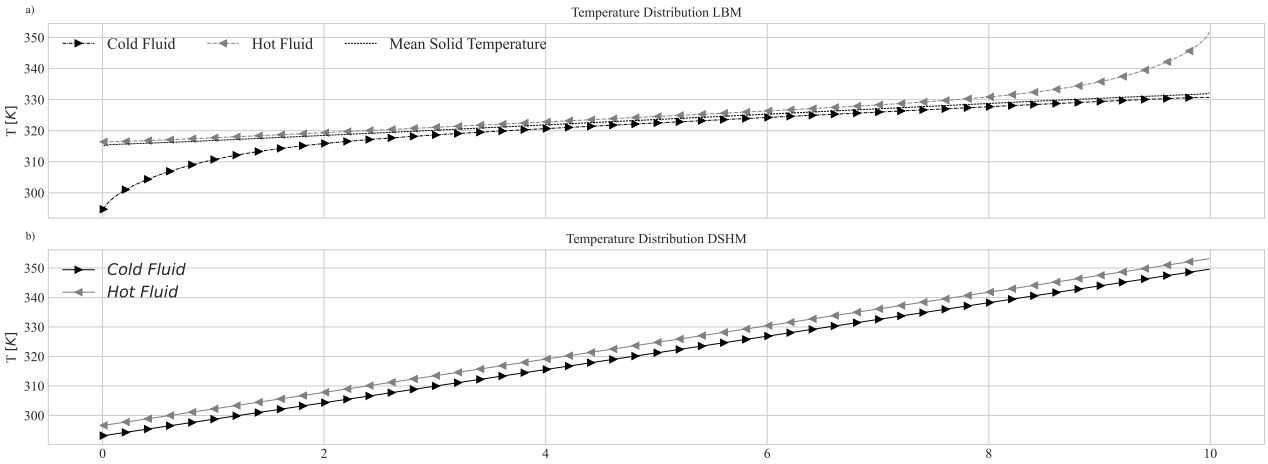

Figure 6. Copper Wall - $u_{in} = 0.001\ ms^{-1}$: a) LBM; b) DSHM.

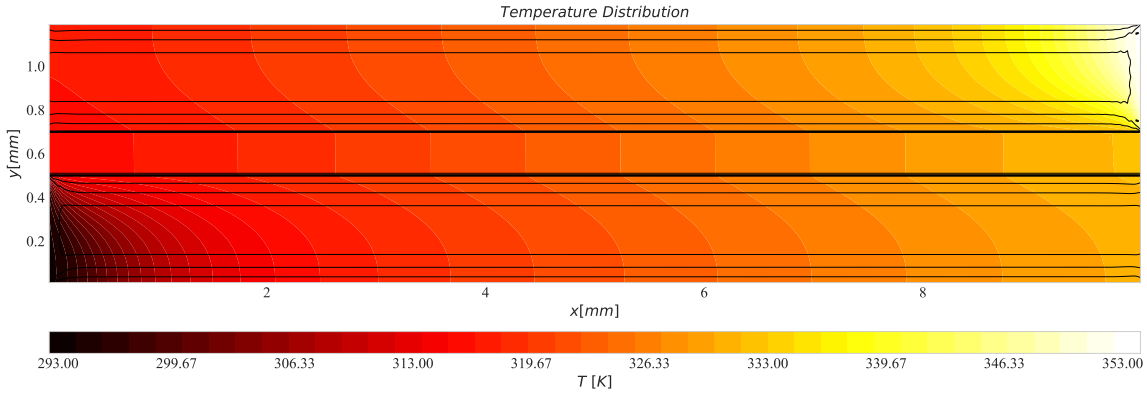

Figure 7. Copper Wall - $u_{in} = 0.001\ ms^{-1}$: 2D Temperature Distribution

able to naturally capture phenomena such as thermal and hydrodynamic no-developed flows at entrance region, and the longitudinal conductive heat transfers thorough the heat exchangers walls.

5. ACKNOWLEDGEMENTS

The authors acknowledge the support received from the CAPES (Coordenação de Aperfeiçoamento de Pessoal de Nível Superior – Brasil – Finance Code 001, process 88887.805775/2023-00), FAPESP (São Paulo Research Foundation grants, processes 2016/09509-1, 2022/12257-5 and 2023/02383-6), and CNPq (National Council for Scientific and Technological Development, process 305941/2020-8).

6. REFERENCES

Aakre, S.R., Thoreson, N.J. and Anderson, M.H., 2023a. "Thermal hydraulic characteristics of liquid sodium and supercritical co2 in a diffusion bonded heat exchanger". *Applied Thermal Engineering*, Vol. 226, p. 120173. ISSN 1359-4311. doi:https://doi.org/10.1016/j.applthermaleng.2023.120173. URL `https://www.sciencedirect.com/science/article/pii/S1359431123002028`.

Aakre, S.R., Thoreson, N.J. and Anderson, M.H., 2023b. "Thermal hydraulic characteristics of liquid sodium and supercritical co2 in a diffusion bonded heat exchanger". *Applied Thermal Engineering*, Vol. 226, p. 120173.

Aneesh, A., Sharma, A., Srivastava, A., Vyas, K. and Chaudhuri, P., 2016. "Thermal-hydraulic characteristics and performance of 3d straight channel based printed circuit heat exchanger". *Applied Thermal Engineering*, Vol. 98, pp. 474–482. ISSN 1359-4311. doi:https://doi.org/10.1016/j.applthermaleng.2015.12.046. URL `https://www.sciencedirect.com/science/article/pii/S1359431115014271`.

Bhatnagar, P.L., Gross, E.P. and Krook, M., 1954. "A model for collision processes in gases. i. small amplitude processes in charged and neutral one-component systems". *Physical Review*, Vol. 94, No. 3, pp. 511–525. ISSN 0031-899X.

Bird, R.B., Stewart, W.E. and Lightfoot, E.N., 2002. *Transport Phenomena, 2nd ed.* John Wiley & Sons, Inc.

Chapman, S. and Cowling, T.G., 1952. *The Mathematical Theory of Non-uniform Gases, 2nd ed.* Cambridge University

Press.

Chen, S., Yan, Y. and Gong, W., 2017. "A simple lattice boltzmann model for conjugate heat transfer research". *International Journal of Heat and Mass Transfer*, Vol. 107, pp. 862–870. ISSN 0017-9310.

Cong, T., Wang, Z., Zhang, R., Wang, B. and Zhu, Y., 2021. "Thermal-hydraulic performance of a pche with sodium and sco2 as working fluids". *Annals of Nuclear Energy*, Vol. 157, p. 108210.

Guo, Z. and Shu, C., 2013. *Lattice Boltzmann Method and its Applications in Engineering*. World Scientific Publishing Co. Pte. Ltd.

Karani, H. and Huber, C., 2015. "Lattice boltzmann formulation for conjugate heat transfer in heterogeneous media". *Phys. Rev. E*, Vol. 91, p. 023304. doi:10.1103/PhysRevE.91.023304. URL `https://link.aps.org/doi/10.1103/PhysRevE.91.023304`.

Korba, D., Wang, N. and Li, L., 2020. "Accuracy of interface schemes for conjugate heat and mass transfer in the lattice boltzmann method". *International Journal of Heat and Mass Transfer*, Vol. 156, p. 119694. ISSN 0017-9310.

Krüger, T., Kusumaatmaja, H., Kuzmin, A., Shardt, O., Silva, G. and Viggen, E., 2017. *The Lattice Boltzmann Method: Principles and Practice*. Springer International Publishing.

Lee, S.Y., Park, B.G. and Chung, J.T., 2017. "Numerical studies on thermal hydraulic performance of zigzag-type printed circuit heat exchanger with inserted straight channels". *Applied Thermal Engineering*, Vol. 123, pp. 1434–1443.

Lee, T. and Liu, L., 2010. "Lattice boltzmann simulations of micron-scale drop impact on dry surfaces". *Journal of Computational Physics*, Vol. 229, No. 20, pp. 8045–8063.

Li, L., Chen, C., Mei, R. and Klausner, J.F., 2014. "Conjugate heat and mass transfer in the lattice boltzmann equation method". *Phys. Rev. E*, Vol. 89, p. 043308.

Liang, H., Liu, H., Chai, Z. and Shi, B., 2019. "Lattice boltzmann method for contact-line motion of binary fluids with high density ratio". *Physical Review E*, Vol. 99, No. 6, p. 063306.

Lienhard, IV, J.H. and Lienhard, V, J.H., 2020. *A Heat Transfer Textbook*. Phlogiston Press, Cambridge, MA, 5th edition. URL `http://ahtt.mit.edu`. Version 5.10.

Ma, Y., Xie, G. and Hooman, K., 2022. "Review of printed circuit heat exchangers and its applications in solar thermal energy". *Renewable and Sustainable Energy Reviews*, Vol. 155, p. 111933. ISSN 1364-0321. doi:https://doi.org/10.1016/j.rser.2021.111933. URL `https://www.sciencedirect.com/science/article/pii/S1364032121011989`.

Martins, I.T., Alvariño, P.F. and Cabezas-Gómez, L., 2023. "Dimensional lattice boltzmann method for transport phenomena simulation without conversion to lattice units". *arXiv preprint arXiv:2302.04120*.

Nellis, G. and Klein, S., 2008. *Heat transfer*. Cambridge university press.

Qian, Y.H., D'Humieres, D. and Lalleman, P., 1992. "Lattice bgk models for navier-stokes equation". *Europhysics Letters*, Vol. 17, No. 6, pp. 479–484.

Rihab, H., Moudhaffar, N., Sassi, B.N. and Patrick, P., 2016. "Enthalpic lattice boltzmann formulation for unsteady heat conduction in heterogeneous media". *International Journal of Heat and Mass Transfer*, Vol. 100, pp. 728–736. ISSN 0017-9310.

Roe, B., Jaiman, R., Haselbacher, A. and Geubelle, P., 2008. "Combined interface boundary condition method for coupled thermal simulations". *International journal for numerical methods in fluids*, Vol. 57, No. 3, pp. 329–354.

Seta, T., 2013. "Implicit temperature-correction-based immersed-boundary thermal lattice boltzmann method for the simulation of natural convection". *Physical Review E*, Vol. 87, p. 063304.

Succi, S., 2001. *The lattice Boltzmann equation: for fluid dynamics and beyond*. Oxford university press.

Zhang, J., Yang, C. and Mao, Z.S., 2012. "Unsteady conjugate mass transfer from a spherical drop in simple extensional creeping flow". *Chemical engineering science*, Vol. 79, pp. 29–40.